

IMPORTANCE OF NUMERICAL EFFICIENCY FOR REAL TIME CONTROL OF TRANSIENT GRAVITY FLOWS IN SEWERS

ARTURO S. LEON¹, MOHAMED S. GHIDAOU²,
ARTHUR R. SCHMIDT³ and MARCELO H. GARCIA⁴

¹ Ph.D. Student, Dept. of Civil and Environmental Engineering,
University of Illinois, Urbana, Illinois 61801, USA. (e-mail: asleon@uiuc.edu)

² Associate Professor, Dept. of Civil Engineering, The Hong Kong University of Science
and Technology, Hong Kong. (e-mail: ghidaoui@ust.hk)

³ Research Assistant Professor, Dept. of Civil and Environmental Engineering,
University of Illinois, Urbana, IL 61801, USA. (e-mail: aschmidt@uiuc.edu)

⁴ Professor and Director of the Ven Te Chow Hydrosystems Lab., Dept. of Civil and
Envir. Eng., University of Illinois, Urbana, IL 61801, USA. (e-mail: mhgarcia@uiuc.edu)

Abstract

Numerical efficiency—achieving a given level of accuracy with the least Central Processing Unit (CPU) time—is of paramount importance in transient flow modeling of sewerage systems. This is particularly important (i) for large sewerage systems containing a wide range of flow controls such as gates and pumps and/or (ii) for systems requiring real-time flow model for their operation. The Tunnel and Reservoir Plan (TARP), which was adopted by the Metropolitan Water Reclamation District of Greater Chicago in 1972 to address the combined sewer overflow (CSO) pollution and flooding problems in the Chicago-land area, is an example of systems requiring a highly efficient transient model. In this paper, the accuracy and efficiency of two second-order explicit Finite-Volume Godunov-Type Schemes (GTS) and one fixed-grid Method of Characteristics (MOC) scheme with space-line interpolation are investigated using problems whose solution contain features that are relevant to transient flows in sewers such as shocks and expansion waves. The results show that the two GTS schemes are significantly faster to execute than the MOC scheme, and in some cases, the accuracy produced by the two GTS schemes can not be matched by the accuracy of the MOC scheme, even when a Courant number close to one and a large number of grids is used. Furthermore, unlike the MOC solutions, which exhibit increasing numerical dissipation with decreasing Courant numbers, the resolution of the shock fronts was maintained by the GTS schemes even for very low Courant numbers.

Keywords: Sewers; Transient flows; Gravity flows; Riemann problem; Godunov schemes; Numerical efficiency; Accuracy; Real time control

1. INTRODUCTION

Numerical efficiency is of paramount importance for successful implementation of real-time control in sewer systems, in which, to reproduce the formation and propagation of hydraulic transients, typically small simulation time steps and a large number of grids are needed. For a given grid size and Courant number, one scheme can be more accurate than another, but not necessarily more efficient numerically. A comparison of numerical efficiency requires measuring the CPU time needed by each of the schemes to achieve the same level of accuracy [e.g., Zhao and Ghidaoui (2004)].

Unsteady gravity flows in sewers have been traditionally modeled by numerically solving the one-dimensional equations of continuity and momentum. Commonly used models range in sophistication from kinematic wave to full dynamic wave solution of these equations (Yen 2001). Most of the models that solve these equations at the level of the full dynamic wave use an implicit finite-difference scheme when the formation of transients is secondary to issues such as conveyance capacity. However, most of the models developed primarily to examine the formation of hydraulic transients use schemes based on the Method Of Characteristics (MOC). The MOC transforms the partial differential equations of continuity and momentum into a set of ordinary differential equations that are relatively easy to solve. As a result, many methods and strategies have been developed to apply the MOC to one-dimensional flows. Among the benefits of these schemes and strategies are methods to incorporate complex boundary conditions into MOC solutions.

Godunov Type Schemes (GTS) for the solution of shallow water equations have been the subject of considerable research (e.g., Alcrudo et al. 1992; Toro 2001). In these schemes, space is discretised into volumes, more often called cells, hence the general term of Finite Volume (FV) method. The numerical solution is not characterized by its value at a set of (discrete) points but by its average over the cells. The evolution of the solution in a given cell is determined by the exchange (via fluxes) at the interfaces with all the neighboring cells. In the Godunov approach, the fluxes are computed by solving Riemann problems at the interfaces between the cells. The powerful character of this approach lies in that the exchange between the fluxes can be computed even if the solution is initially discontinuous or if it becomes so at later times (Guinot 2003). The boundary conditions for the GTS schemes can be treated in a similar way to the MOC.

The purpose of this paper is to contrast the numerical efficiency produced by one MOC scheme, which is currently the scheme most used to examine the formation of hydraulic transients and two second-order (in space and time) GTS schemes. Second order accuracy in space and time for the GTS schemes is obtained by using a Monotone Upstream-centred Scheme for Conservation Laws (MUSCL) reconstruction in conjunction with a Hancock two-stage scheme for advancing the cell average solution from one time level to the next (e.g., Toro 2001). The difference among the considered GTS schemes is only in the method used to solve the Riemann problem. The first GTS scheme uses the Guinot Riemann solver credited to Guinot (2003) and the second one uses the HLL Riemann solver attributed to Harten, Lax and Van Leer (Toro 2001). This paper is organized as follows: First, the governing equations

in conservative form for one-dimensional shallow water equations are presented. Second, the accuracy and efficiency of two GTS schemes and one MOC scheme are investigated using problems whose solution contain features that are relevant to transient flows in sewers. Last, the results are summarized in the conclusion.

2. GOVERNING EQUATIONS

One-dimensional open channel flow continuity and momentum equation for non-prismatic channels or rivers may be written in its vector conservative form as follows (Chaudhry 1987):

$$\frac{\partial \mathbf{U}}{\partial t} + \frac{\partial \mathbf{F}}{\partial x} = \mathbf{S} \quad (1)$$

where the vector variable \mathbf{U} , the flux vector \mathbf{F} and the source term vector \mathbf{S} are given respectively by:

$$\mathbf{U} = \begin{bmatrix} A \\ Q \end{bmatrix}, \quad \mathbf{F} = \begin{bmatrix} Q \\ \frac{Q^2}{A} + \frac{A\bar{p}}{\rho} \end{bmatrix} \text{ and } \mathbf{S} = \begin{bmatrix} 0 \\ F_w + (S_0 - S_f)gA \end{bmatrix} \quad (2)$$

where A = cross-sectional area of the channel; Q = flow discharge; \bar{p} = average pressure of the water column over the cross sectional area; ρ = liquid density; g = gravitational acceleration; S_0 = slope of the bottom channel; S_f = slope of the energy line, which may be estimated using an empirical formula such as the Manning's equation; and F_w = momentum term arising from the longitudinal variation of the channel width. For a circular cross-section channel (Fig. 1), F_w becomes zero, the hydraulic area is given by $A = d^2/8(\theta - \sin \theta)$, the hydraulic radius by $R = d/4(1 - \sin \theta/\theta)$, and the term $A\bar{p}/\rho$ contained in the flux term \mathbf{F} in Eq. (2) is given by

$$\frac{A\bar{p}}{\rho} = \frac{g}{12} \left[(3d^2 - 4dy + 4y^2) \sqrt{y(d-y)} - 3d^2(d-2y) \arctan \frac{\sqrt{y}}{\sqrt{d-y}} \right] \quad (3)$$

where d is the diameter of the circular cross-section channel and y is the water depth.

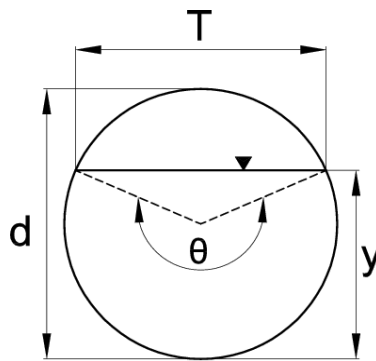


Fig. 1 Definition of variables in circular cross-sections

3. TESTS OF ACCURACY AND NUMERICAL EFFICIENCY

The objective of this section is to evaluate the accuracy and efficiency of two second-order GTS schemes and one MOC scheme using two problems whose solution contain features that are relevant to transient flows in sewers.

For convenience, the grid size, Courant number (Cr), Manning roughness coefficient (n) and channel slope (S_0) used in each example are indicated in the relevant figures and thus will not be repeated in the text. Furthermore, the CPU times that are reported in this paper were averaged over three realizations and computed using a Pentium IV 3.20 GHz personal computer.

3.1 TEST 1

This test is used to compare the accuracy and numerical efficiency of the two GTS schemes and the MOC scheme with space-line interpolation. The test rig consists of a sudden opening of a gate separating two pools of still water with different depths mid-way of a 1000 m long sewer with a diameter of 15 m. A zero water flux at the boundaries is used in the analysis, namely $Q(0,t) = 0$ and $Q(1000,t) = 0$. The initial conditions are:

$$\begin{cases} y = 10.0 \text{ m} & \text{and } u = 0.0 \text{ m/s for } x \leq 500 \text{ m} \\ y = 3.0 \text{ m} & \text{and } u = 0.0 \text{ m/s for } x > 500 \text{ m} \end{cases}$$

A quantitative measure of the numerical dissipation can be obtained by using the integral form of the energy equation (Karney 1990, Ghidaoui and Cheng 1997, Zhao and Ghidaoui 2004). This equation in open channel flows for a control volume of length L can be written as (Ghidaoui et al. 1997):

$$\frac{d}{dt} \int_0^L \frac{u^2}{2} A dx + \frac{d}{dt} \int_0^L g \bar{y} A dx + \int_0^L g u (S_f - S_0) A dx + Q \left(\frac{u^2}{2} \Big|_0^L \right) + Q \left(g y \Big|_0^L \right) = 0 \quad (4)$$

Where \bar{y} is the vertical distance from the sewer invert to the centroid of the hydraulic area, and t is the time. The total energy within the control volume at a given time (E_t) involves the first 2 terms in the left hand side of Eq. 4 (kinetic and potential energy) and it is given by:

$$E_t = \int_0^L \frac{u^2}{2} A dx + \int_0^L g \bar{y} A dx$$

The sewer is assumed to be frictionless and horizontal. The absence of friction and gravity forces and the imposition of zero flux at the boundaries imply that the total energy is conserved throughout the transient. That is, $dE_t/dt = 0$ or $E_t = \text{constant}$. Therefore, any dissipation found in the results is solely due to numerical dissipation.

The ability of the schemes to conserve mass is first tested. Since zero mass flux boundary conditions are used in the current test case, the total mass in the sewer is invariant with time. Whether or not the schemes are able to conserve mass (i.e., keep the total amount of fluid in the sewer invariant with time in this case) is now tested. The simulation results for the water depth versus time at $x = 2.5$ m and the mass traces are shown in Fig. 2 and 3, respectively. The results show that unlike the MOC scheme, the two GTS schemes conserve mass. For instance, Fig. 3 shows that after 400 seconds of simulation, about 20% of the initial total water volume is lost by the MOC scheme and none by the two GTS schemes.

Following, the influence of the Courant number on the accuracy of the schemes before and after the shock and rarefaction waves have interacted with the zero-flux boundaries is investigated. The simulation results are shown in Fig. 4, 5 and 6. The results show that for the same Courant number, the numerical dissipation exhibited by the two GTS schemes is

significantly smaller than the one produced by the MOC scheme. Furthermore, unlike the MOC scheme, the two GTS schemes do not significantly reduce their resolution when decreasing the Courant number. The results also show that the jump simulated by the MOC scheme is slower than the actual jump. The accurate prediction of the speed of the jumps in sewer systems is very important because it dictates the right timing at which surcharging occurs.

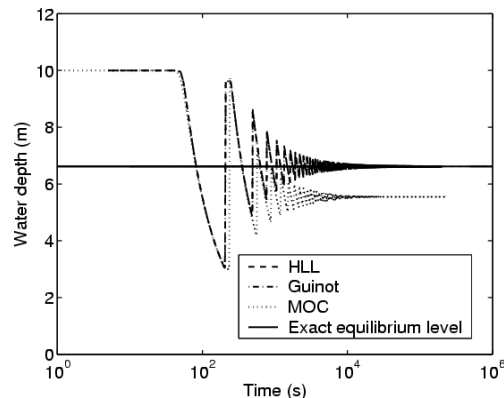


Fig. 2 Water depth versus time at $x = 2.5$ m for test No 1 ($\Delta x = 5.0$ m, $Cr = 0.3$, $S_f = 0$, $S_0 = 0$)

Recall that the total energy (sum of kinetic and potential) in the channel reach is invariant with time (i.e., $E(t)/E_0 = 1$). Fig. 7 shows the relative energy traces $E(t)/E_0$ for different Courant numbers. This figure demonstrates that unlike the MOC scheme, the numerical dissipation exhibited by the two GTS schemes is not sensitive to the Courant number. This figure also shows that for a given Courant number, the numerical dissipation produced by the two GTS schemes is significantly smaller than the one obtained by the MOC scheme. For instance, when $Cr = 0.3$, after 400 seconds of simulation, more than 40% of the initial total energy is dissipated by the MOC approach and only about 20% by both GTS schemes.

To this point, it is shown that for the same grid size and for the same Courant number, the two GTS schemes are more accurate than the MOC scheme with space-line interpolation. However, as pointed out by Zhao and Ghidaoui (2004), a comparison of the numerical efficiency requires measuring the CPU time needed by each of the schemes to achieve the same level of accuracy.

To compare the efficiency of these schemes, before and after the shock and rarefaction waves have interacted with the zero-flux boundaries, the numerical dissipation against the number of grids is plotted on log-log scale and shown in Fig. 8 and 9. Fig. 8 (before the shock and rarefaction waves have interacted with the zero-flux boundaries) shows that the numerical dissipation is linearly (on log log scale) reduced when the number of grids is increased. However, when convergence is close to being achieved, the reduction of the numerical dissipation asymptotically tends to zero. In real-time simulations (due to the computational cost), the accuracy pursued in the numerical modeling will typically result in the linear portion of Fig. 8. Hence, the linear relationships are used for the comparison of numerical efficiency. These linear relationships were fitted to power functions which equations are

shown in this same figure. Using these equations, the number of grids needed by each of the schemes to achieve two different levels of accuracy were computed. These in turn were used to compute the CPU times. These results are presented in Table 1. Although the curves in Fig. 8 and the equations of these curves (also given in Fig. 8) were obtained before the shock and rarefaction waves have interacted with the zero-flux boundaries (first interaction with the boundaries occur after about 50 seconds), to get significant CPU times, the simulation time was arbitrarily extended to 10000 seconds. Notice in this table that the two GTS schemes have similar efficiency. Also note that to achieve the same degree of accuracy, the MOC approach requires a much finer grid size than the two GTS methods. In addition, this table shows that to achieve the specified level of accuracy, the two GTS schemes are about 100 to 300 times faster to execute than the MOC approach. This clearly shows the advantage of GTS schemes over the MOC scheme for real time control.

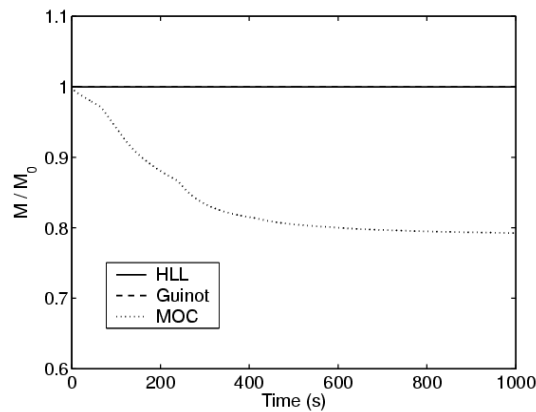


Fig. 3 Mass traces for test No 1 ($\Delta x = 5.0$ m, $Cr = 0.3$, $S_f = 0$, $S_0 = 0$)

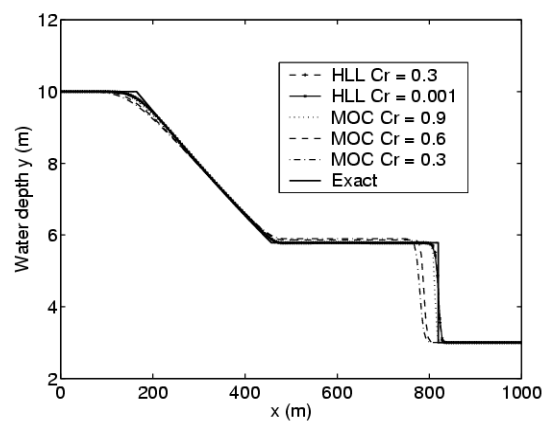


Fig. 4 Water depth profile for test No 1 before the shock and rarefaction waves have interacted with the zero-flux boundaries ($\Delta x = 5.0$ m, $t = 36$ s, $S_f = 0$, $S_0 = 0$)

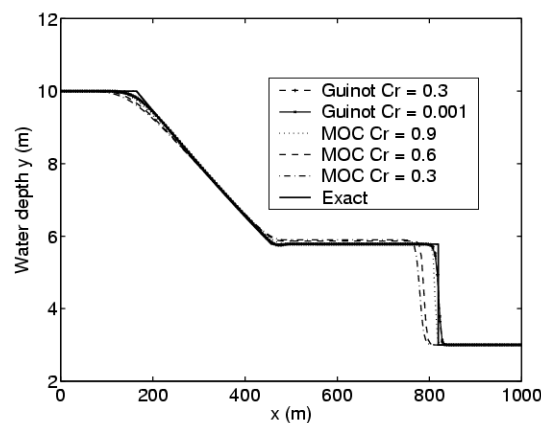


Fig. 5 Water depth profile for test No 1 before the shock and rarefaction waves have interacted with the zero-flux boundaries ($\Delta x = 5.0$ m, $t = 36$ s, $S_f = 0$, $S_0 = 0$)

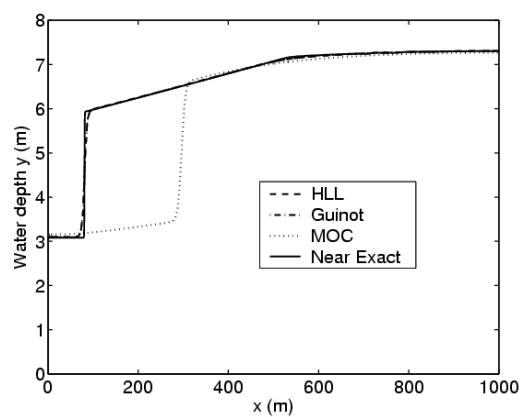


Fig. 6 Water depth profile for test No 1 after about one wave cycle ($\Delta x = 5.0$ m, $Cr = 0.3$, $t = 197$ s, $S_f = 0$, $S_0 = 0$)

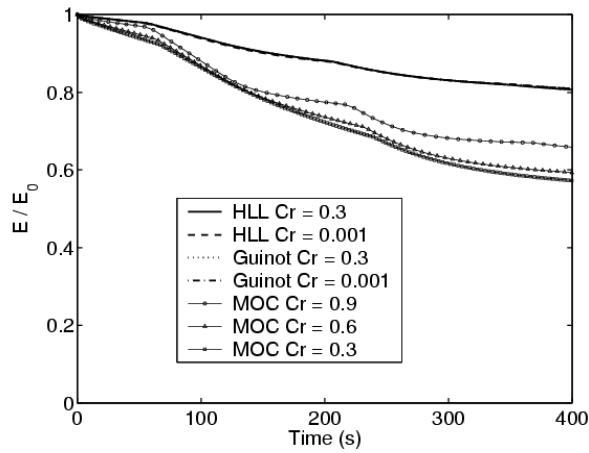


Fig. 7 Energy traces for test No 1 ($\Delta x = 5.0$ m, $S_f = 0, S_0 = 0$)

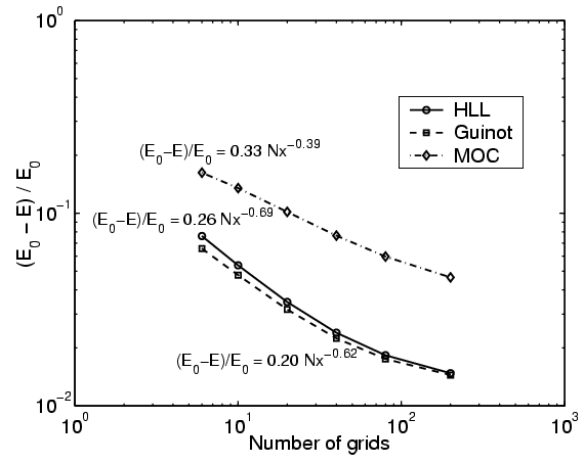


Fig. 8 Relation between numerical dissipation and number of grids for test No 1 before the shock and rarefaction waves have interacted with the zero-flux boundaries ($Cr = 0.3, t = 36$ s, $S_f = 0, S_0 = 0$)

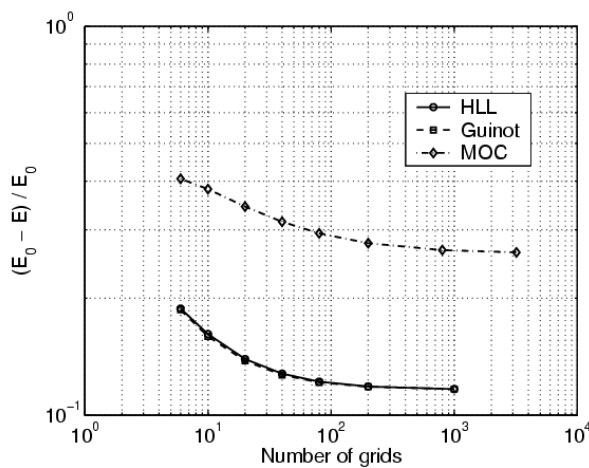


Fig. 9 Relation between numerical dissipation and number of grids for test No 1 after about one wave cycle ($Cr = 0.3, t = 200$ s, $S_f = 0, S_0 = 0$)

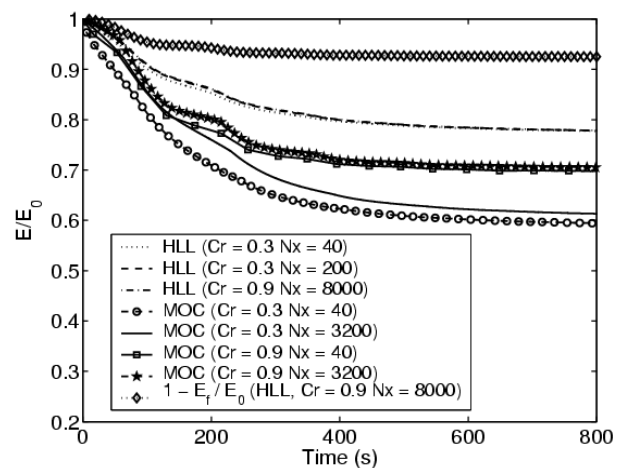


Fig. 10 Energy traces for test No 2 ($n = 0.015, S_0 = 0$)

Table 1. Comparison of efficiency among the two GTS methods and the MOC scheme with space-line interpolation ($Cr = 0.3, t = 10000$ s, $S_f = 0, S_0 = 0$) [Nx is number of grids needed to achieve a specified level of accuracy]

Description		HLL	Guinot	MOC
$(E_0 - E)/E_0 = 2\%$	Nx	42	42	1324
	CPU time (s)	2.44	2.55	819.2
$(E_0 - E)/E_0 = 3\%$	Nx	23	22	468
	CPU time (s)	0.83	0.73	104.2

The results after one wave cycle (Fig. 9) show that the accuracy produced by the two GTS schemes can not be matched by the accuracy of the MOC scheme, even when using a large number of grids. The poor results obtained with the MOC scheme may be explained by recalling that this scheme does not conserve mass. At $t = 0$, the initial total energy (E_0) is only potential. After the flow has reached to a static equilibrium ($t = \infty$), the kinetic energy is zero and the total energy is again only potential. If mass is conserved, the potential energy at $t = \infty$ is 77.1% of E_0 , which means that the maximum energy that can be dissipated in the system is 22.9% of E_0 . Any additional energy loss is a result of a numerical loss of mass in the simulation. The inability of the MOC scheme to conserve mass can produce dissipations beyond the maximum energy that can be dissipated (22.9%), as can be observed in Fig. 7. In this figure for instance, when $Cr = 0.3$, after 400 s of simulation time, the MOC scheme has produced a numerical dissipation of more than 40%, about half of which can be attributed to the numerical loss of water mass (Fig. 3). The situation is noticeably improved when the Courant number is increased to a value close to one and a large number of grids is used. However in this particular case, these improvements were not enough to match the accuracy of the GTS schemes.

3.2 TEST 2

This test is used (1) to investigate and compare the accuracy and efficiency of the two GTS schemes and the MOC method with space-line interpolation in the presence of friction, and (2) to measure the relative magnitude of the numerical and physical dissipation. The parameters for this test case are the same than the previous one except friction is included using a Manning roughness coefficient of 0.015.

Because it is shown that the two GTS schemes have similar accuracy and efficiency, only the GTS scheme with HLL Riemann solver is considered in this test case. Since the energy dissipation in this case is only due to friction (E_f), the remaining energy after a given period can be obtained by subtracting E_f attained during that period from the initial energy E_0 . E_f may be obtained by integration of the net work done by the force of friction over a given period.

The simulation results for the relative energy traces for different numbers of grids and Courant numbers is presented in Fig. 10. The results for the GTS scheme show that for the same Courant number (e.g., $Cr = 0.3$), the numerical dissipation is slightly reduced when the number of grids is increased (e.g., 200 instead of 40). However, when convergence is close to being achieved, the solution is independent of the number of grids used (e.g., compare the solution obtained with 200 and 8000 grids). Regarding to the influence of the Courant number in the solution, it was pointed out previously that the two GTS schemes are not sensitive to this parameter. To determine if the dissipation produced by the GTS scheme is only physical, the traces of $1 - E_f/E_0$ and E/E_0 were compared for the HLL scheme with $Cr = 0.9$ and $N_x = 8000$. Fig. 10 shows that these traces are notably different and consequently part of the total dissipation produced by the GTS scheme is numerical. Since numerical dissipation is present, it is expected that the actual physical dissipation be greater than the value computed for E_f .

For instance, after 400 s of simulation time, the computed values of E / E_0 and $1 - E_f / E_0$ are about 0.80 and 0.93, respectively. The total dissipation in this case is about 20%, the actual physical dissipation is not about 7% but a value significantly greater and consequently the numerical dissipation is considerably smaller than 13%.

In the case of the MOC scheme, the results show that for the same number of grids, the dissipation produced is highly dependent on the Courant number. When using a larger number of grids, the numerical dissipation is reduced but not enough to overcome the effect of a small Courant number. The results also show that after the first quarter wave cycle (about 50 s), the accuracy produced by the GTS scheme can not be matched by the accuracy of the MOC scheme, even when using a Courant number close to one and a large number of grids. In this case, the physical dissipation is totally overwhelmed by the numerical dissipation. The reasons for the poor results obtained with the MOC scheme are similar to the discussed in Test 1.

4. CONCLUSIONS

In this paper the accuracy and efficiency of two GTS schemes and one MOC scheme were investigated using problems whose solution contain features that are relevant to transient flows in sewers such as shock and expansion waves. The key results are as follows:

1. FV formulation ensures that the two GTS schemes conserve mass and momentum. The fixed-grid MOC scheme with space-line interpolation does not conserve mass for Courant numbers less than one.
2. The GTS methods can handle boundary conditions in a similar way to the MOC scheme.
3. The GTS schemes do not significantly reduce their resolution when decreasing the Courant number as does the MOC scheme with space-line interpolation.
4. Numerical tests show that to achieve a given level of accuracy, the two GTS methods are significantly faster to execute than the fixed-grid MOC scheme with space-line interpolation, and in some cases, the accuracy produced by the two GTS schemes can not be matched by the accuracy of the MOC scheme, even when a Courant number close to one and a large number of grids is used. Thus, for real time control, GTS schemes must be preferred over MOC schemes.

ACKNOWLEDGEMENTS

The authors would like to acknowledge the Metropolitan Water Reclamation District of Greater Chicago for their financial support of this research.

REFERENCES

- Alcrudo, F., Garcia-Navarro, P., and Saviron, J-M. (1992). "Flux-difference splitting for 1D open channel flow equations." *Int. J. for Numerical Methods in Fluids*, Vol. 14, pp. 1009-1018.
- Chaudhry, M. H. (1987). *Applied hydraulic transients*, Van Nostrand Reinhold, New York.

- Ghidaoui, M. S., and Cheng, Y. P. H. (1997). "Energy equation in unsteady open channel flows: Formulation and Application." *Advances in Comput. Eng. Science*, pp. 582-587.
- Guinot, V. (2003). *Godunov-type schemes*, Elsevier Science B.V., Amsterdam, The Netherlands.
- Karney, B. W. (1990). "Energy relations in transient closed-conduit flow." *J. Hydraul. Eng.*, Vol. 116(10), pp. 1180-1196.
- Toro, E. F. (2001). *Shock-capturing methods for free-surface shallow flows*, Wiley, LTD, Chichester, U.K.
- Yen, B. C. (2001). *Hydraulics of sewer systems*, in stormwater collection systems design Handbook, McGraw-Hill.
- Zhao, M., and Ghidaoui M. S. (2004). "Godunov-type solutions for water hammer flows." *J. Hydraul. Eng.*, Vol. 130(4), pp. 341-348.